

Laser-driven formation of a high-pressure phase in amorphous silica

ALBERTO SALLEO^{*1,2,†}, SETH T. TAYLOR^{1,3,‡}, MICHAEL C. MARTIN⁴, WENDY R. PANERO^{5,§},
RAYMOND JEANLOZ⁵, TIMOTHY SANDS^{1,¶} AND FRANÇOIS Y. GÉNIN²

¹Department of Materials Science and Engineering, University of California Berkeley, Berkeley, California 94720, USA

²Lawrence Livermore National Laboratory, 7000 East Avenue, Livermore, California 94550, USA

³National Center for Electron Microscopy, Lawrence Berkeley National Laboratory, 1 Cyclotron Road, Berkeley, California 94720-8226, USA

⁴Advanced Light Source Division, Lawrence Berkeley National Laboratory, 1 Cyclotron Road, BLDG 6R2100, Berkeley, California 94720-8226, USA

⁵Department of Earth and Planetary Science, University of California Berkeley, Berkeley, California 94720, USA

[†]Present address: Palo Alto Research Center, 3333 Coyote Hill Road, Palo Alto, California 94304, USA

[‡]Present address: GE Global Research, One Research Circle, Niskayuna, New York 12309, USA

[§]Present address: Department of Geological Sciences, University of Michigan, Ann Arbor, Michigan 48109, USA

[¶]Present address: School of Materials Engineering and School of Electrical & Computer Engineering, West Lafayette, Indiana 47907, USA

*e-mail: asalleo@parc.com

Published online: 2 November 2003; doi:10.1038/nmat1013

Because of its simple composition, vast availability in pure form and ease of processing, vitreous silica is often used as a model to study the physics of amorphous solids. Research in amorphous silica is also motivated by its ubiquity in modern technology, a prominent example being as bulk material in transmissive and diffractive optics for high-power laser applications such as inertial confinement fusion (ICF)^{1,2}. In these applications, stability under high-fluence laser irradiation is a key requirement³, with optical breakdown occurring when the fluence of the beam is higher than the laser-induced damage threshold (LIDT) of the material³. The optical strength of polished fused silica transmissive optics is limited by their surface LIDT³. Surface optical breakdown is accompanied by densification⁴, formation of point defects⁵, cratering, material ejection, melting and cracking³. Through a combination of electron diffraction and infrared reflectance measurements we show here that synthetic vitreous silica transforms partially into a defective form of the high-pressure stishovite phase under high-intensity (GW cm^{-2}) laser irradiation. This phase transformation offers one suitable mechanism by which laser-induced damage grows catastrophically once initiated, thereby dramatically shortening the service lifetime of optics used for high-power photonics.

Fused silica is used for transmissive optics in ICF facilities because, of all candidate materials with suitable optical properties, it currently can be manufactured in large components and has a high LIDT at 355 nm. Some degree of optical damage is however inevitable as large aperture (~ 0.5 m) components cannot be manufactured free of flaws.

Successive irradiation of existing laser-induced damage sites causes catastrophic damage to propagate at fluences lower than the original LIDT⁶: initial microscopic damage sites eventually grow to a macroscopic size under repetitive irradiation determining the failure of the optical element. Such behaviour must be triggered by enhanced coupling between light and the glass, for instance due to the formation of micro-cracks at the damage site⁷. Although damage induced in silica

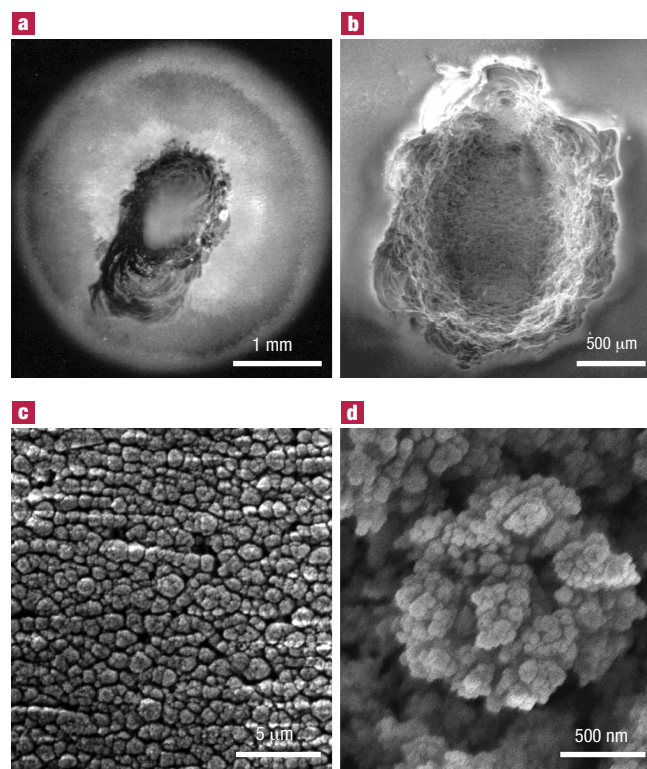


Figure 1 Images of the laser-damaged surface of polished fused silica windows. **a**, Reflected light micrograph and **b**, SEM micrograph of the drilled hole. **c**, **d**, SEM micrographs of the material redeposited around the drilled hole.

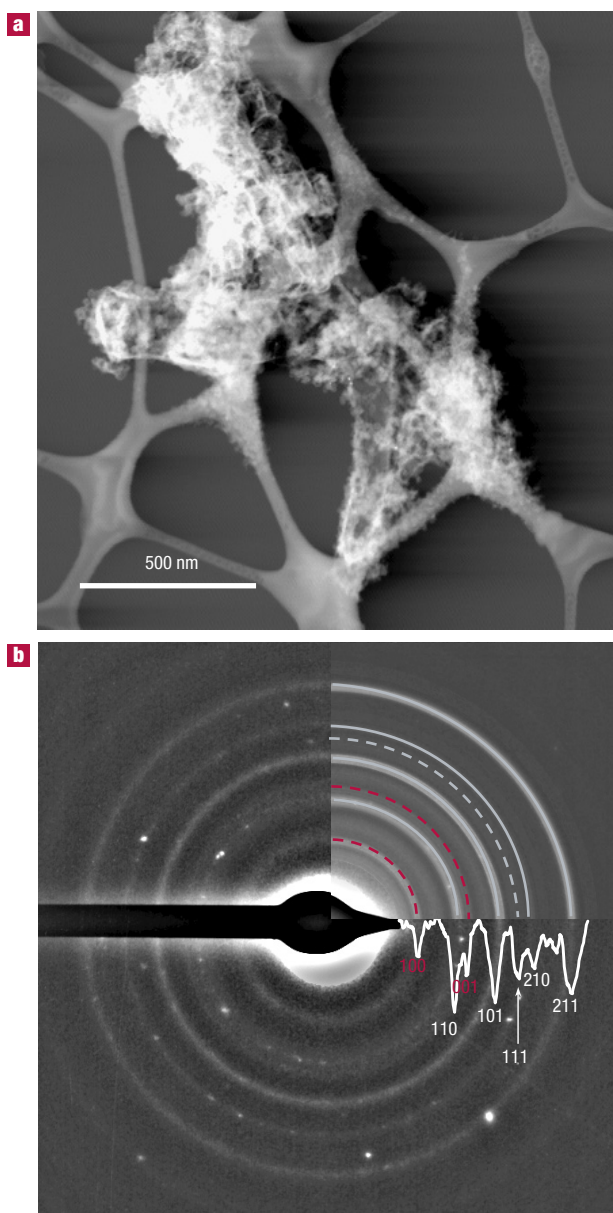


Figure 2 A crystalline particle of the deposited material after HF etching. **a**, STEM micrograph. **b**, Ring diffraction pattern; the top-right corner is the result of circular averaging of the pattern. The diffraction rings that are forbidden in non-defective stishovite are in red. The diffraction rings indicated with dashed lines are extremely weak with the exception of a few bright spots. A lineout through the scanned diffraction pattern is included.

by laser pulses longer than a few tens of picoseconds is generally believed to occur through conventional heat deposition at defects⁸, the possibility of laser-induced phase transformations in the material under repetitive irradiation has never been thoroughly investigated.

The structure of most SiO₂ polymorphs, both crystalline and amorphous, is based on tetrahedral units of silicon coordinated to four oxygen atoms. At pressures above 7 GPa, the stable polymorph is stishovite, in which silicon is sixfold-coordinated⁹. Correspondingly, in the 10–20 GPa pressure range, the coordination in glasses increases from 4 to 6 (ref. 10). At higher pressures, the formation of post-stishovite phases has been observed where Si is octahedrally coordinated.

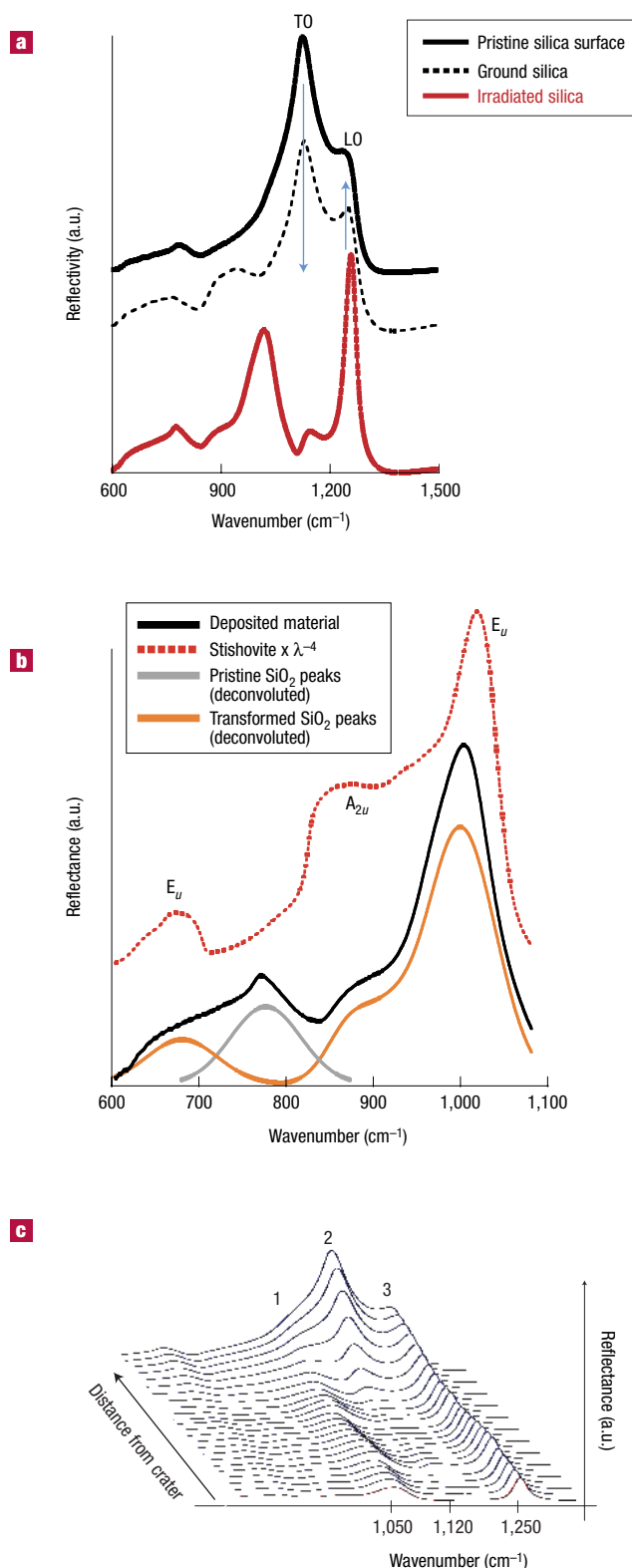
Polished fused silica windows were laser-damaged on the front surface. Scanning electron microscopy (SEM) was carried out on the damaged surface. Redeposited material surrounding the damage site hole (Fig. 1c,d) was collected from the surface and prepared for transmission electron microscopy (TEM) characterization (Fig. 2). Further characterization was performed by collecting the infrared reflection spectrum of the deposited material and comparing it to the spectra of an unirradiated surface, a pellet of synthetic stishovite, and ground silica powder (Fig. 3).

The diameter of the damage hole is roughly equivalent to the laser-beam diameter (Fig. 1a,b). The hole has vertical walls and a flat bottom. This profile indicates that the damage hole is due to optical ablation of the transparent material rather than to subsurface explosion and subsequent material ejection, where shock-wave dynamics would typically lead to a conical crater. The material surrounding the hole is a uniform aggregate of small, rounded particles, some of which are of the order of 10 nm or smaller in diameter (Fig. 1c,d). The size and morphology of the material surrounding the hole indicates that it is the result of condensation from the laser-induced plasma and not ejection from the hole in the solid state.

The electron-diffraction pattern from material adjacent to the hole indicates clearly the presence of small crystallites (Fig. 2b). We compared the experimental diffraction pattern to all known high-pressure SiO₂ polymorphs (coesite, stishovite and post-stishovite phases)^{11–17}. The overall best agreement of all SiO₂ polymorphs is found with stishovite (Table 1). It must be noted, however, that although many post-stishovite polymorphs have been experimentally found, it has been postulated¹⁸ that a virtually infinite number of them may exist and be metastable as they are all derived through slight variations of a common parent structure. The diffraction rings are weak and diffuse, indicating that the crystallites are defective. The 100 and 001 reflections, which are normally forbidden for tetragonal stishovite, are observed here as faint rings (Fig. 2b). The presence of 100 and 001 reflections in addition to the relatively large width of the diffraction rings provide evidence that a substantial fraction of the crystal population departs from the ideal crystal structure due to either the presence of defects or permanent deformation.

Further characterization of the deposited material was performed by infrared reflection spectroscopy (Fig. 3a,b). The infrared spectrum of the deposited material is the result of two simultaneous alterations of the glass surface: the appearance of a new phase and the pulverization of the material into small particles. Infrared reflectance data confirm the presence of significant amounts of octahedrally coordinated material as well as defective tetrahedral SiO₂ throughout the entire layer of deposited material. The low-frequency part of the infrared reflectance spectrum with its deconvolution is shown in Fig. 3b. In the deconvolution, we separated the peaks present in the pristine silica surface from the peaks appearing in the transformed material. The spectrum of the transformed material is compared with that of a bulk sample of synthetic stishovite in Fig. 3b. The laser-irradiated material consists of particles much smaller than the infrared wavelength (Fig. 1c,d). The stishovite spectrum is thus multiplied by λ^{-4} (where λ is the wavelength) in order to normalize for Rayleigh-scattering modulation occurring in the deposited material. The strong peak at 1,020 cm⁻¹ in the spectrum of the deposited material is located in a spectral region where no signal from tetrahedrally coordinated SiO₂ polymorphs exists, and it is in good agreement with the longitudinal optical (LO) component of the high-frequency E_u vibration of stishovite⁹. The 670 cm⁻¹ peak corresponds to the LO component of the low-frequency E_u vibration of stishovite. The broad band at 900 cm⁻¹ is the superposition of the LO component of the A_{2u} stishovite vibration and the Si-OH dangling bond vibration¹⁹ that appears in the ground silica spectrum as well (Fig. 3a). Other changes in the reflectance spectrum are due to the enhancement of the LO bands caused by the pulverization of the material after irradiation. The infrared reflectance

Figure 3 Infrared reflectance spectra of the deposited material. **a**, Spectra of the pristine surface, ground silica powder and redeposited material (a.u. = arbitrary units). The main features of the infrared reflection spectrum of fused silica are a peak centred around 790 cm^{-1} attributed to Si–O–Si rocking motion and a strong peak at $1,123\text{ cm}^{-1}$ with a shoulder at $1,236\text{ cm}^{-1}$ due to the splitting of the LO and TO components of the asymmetric stretching of tetrahedral Si–O units. The broad band at 900 cm^{-1} in the spectrum of ground silica powder is assigned to dangling Si–OH bonds created during comminution¹⁹, as confirmed by its presence in the spectra of sol–gel-processed SiO_2 . **b**, Deconvolution of the low-frequency part of the spectrum of the redeposited material. Si–O vibrations from the pristine surface and from the transformed material are indicated in the figure. **c**, Spatial mapping by infrared reflective spectroscopy of the area covered with deposited material. Scanning was performed in $100\text{-}\mu\text{m}$ steps starting at the edge of the crater, where the density of deposited particles is highest. Peak 1 is the LO component of the high-frequency E_u vibration of the octahedral Si–O bond. Peaks 2 and 3 are, respectively, the TO and LO component of the asymmetric stretching of the tetrahedral Si–O bond. The features of the infrared spectrum due to laser irradiation smoothly disappear as the distance from the crater increases until the original spectrum of the glass surface is recovered.



spectrum of the deposited material is the result of both direct illumination and multiple scattering between particles. The resulting oblique illumination^{9,20} in addition to the electric field distribution in particle/matrix composites²¹—when the particles are smaller than the wavelength—are known to cause enhancement of LO modes ($1,250\text{ cm}^{-1}$ for tetrahedral SiO_2 and $1,020\text{ cm}^{-1}$ for octahedral SiO_2) compared with the transverse optical (TO) modes ($1,123\text{ cm}^{-1}$ for tetrahedral SiO_2 and 850 cm^{-1} for octahedral SiO_2). The LO enhancement and the TO decrease due to the presence of small particles are confirmed by the spectrum of ground silica powder, albeit to a lesser extent because of the larger particle size, where the LO shoulder at $1,250\text{ cm}^{-1}$ grows in intensity compared with the main peak in the stretching band (TO component) and starts emerging as a separate peak (Fig. 3a). The intensity of the $1,020\text{ cm}^{-1}$ and $1,250\text{ cm}^{-1}$ peaks is correlated with deposited particle density (Fig. 3c): both peaks increase in intensity as spectra are taken progressively closer to the crater edge. Concurrently, the TO component of the tetrahedral SiO_2 stretching vibration ($1,123\text{ cm}^{-1}$) disappears and the overall reflectivity of the surface decreases because of the increased surface roughness. The SEM and TEM analyses and the infrared reflection spectroscopy together show that the deposited material consists of grains a few tens of nanometres in diameter, a fraction of which contains stishovite microcrystallites in a matrix of defective tetrahedral silica glass.

Laser-induced surface breakdown is accompanied by the formation of a plasma in front of the target surface. Because the plasma forms during the pulse, it absorbs the laser energy and partially shields the surface²². Energy is supplied to the plasma during the laser pulse (8.4 ns) when only limited expansion takes place. Therefore, initially the plasma is a hot, partially ionized fluid of near-solid density. We speculate that the octahedral SiO_2 aggregates form in the plasma during or shortly after the laser pulse, before the expansion causes a rapid decrease in density, temperature and pressure of the fluid, bringing about the condensation of the particles on the surface. In similar pressure conditions (for example, shock loading) other crystalline SiO_2 polymorphs, quartz and cristobalite, were observed to form a tetrahedral diaplectic glass^{23,24}. Irreversible transformation of glass into stishovite was observed only when copper particles were added to the initial mixture in order to increase the thermal quenching rate¹⁷. In contrast with shock loading, here the transformation is accompanied by the formation of a high-energy fluid phase and does not necessarily have to proceed through an all-solid-state path, thus favouring the formation of stishovite. This phase transformation has profound effects on the properties of the material, as the coordination change of the central silicon atom is accompanied by an alteration of

the nature of the silicon–oxygen bond from almost purely covalent into partially ionic¹⁰.

Stishovite is customarily formed by shock-loading or by quasi-statically compressing low-pressure SiO_2 phases in an effort to simulate the conditions under which it is formed in nature (for example, planetary interiors or meteorite impacts). In the latter case, the high

Table 1 Interplanar spacings measured from TEM diffraction patterns and spacings of stishovite and α -PbO₂ phase¹³ for various crystallographic planes.

These two phases provided the best match of all SiO₂ polymorphs. Although some reflections match those found in the α -PbO₂ phase, at least two of the strongest reflections from this phase are absent in the experimental pattern.

d_{obs} Part. 1 (Å)	Intensity	d_{hkl} stishovite (Å)	hkl	$ \Delta d $ (%)	d_{hkl} α -PbO ₂ (Å)	hkl	$ \Delta d $ (%)
4.25 ± 0.25	Weak	4.17	100	2	-	-	-
2.9 ± 0.1	Strong	2.96	110	2	3.15	110	7.9
2.68 ± 0.08	Very weak	2.66	001	0.7	2.59	111	3.5
					2.35	020	Missing
2.25 ± 0.08	Strong	2.25	101	0	2.25	002	0
					2.15	200	Missing
2.03 ± 0.05	Very weak	1.98	111	2.5	2.08	021	2.4
					1.99	102	2
1.89 ± 0.06	Strong	1.87	210	1	1.88	121	0.5
1.60 ± 0.05	Strong	1.53	211	4.5	1.58	220	1.3

quenching rate needed to recover the metastable high-pressure phase at ambient conditions is often obtained by laser irradiation at pressure of the glass powders mixed with a radiation absorbing material (for example, Pt shavings). A variation of this method consists of selecting the appropriate laser wavelength where glass itself is the radiation-absorbing material. The high-energy deposition rate generates localized high temperatures and consequently high pressures due to non-equilibrium expansion of the heated areas, as expected according to classical thermomechanics. Using this concept (that is, laser wavelength $\lambda = 10.6 \mu\text{m}$, which is strongly absorbed in the glass and pulsewidths from a few milliseconds to continuous in order to allow high pressures to develop fully), coesite, stishovite and post-stishovite phases have been synthesized from quartz or SiO₂ glass^{25,26}. In the present work on the other hand, the fused silica surface is nominally transparent at the laser irradiation wavelength and energy deposition is due to nonlinear optical breakdown of the surface. During repetitive irradiation, energy deposition may occur through direct coupling with the transformed material. Thus, we show for the first time that laser illumination conditions that are representative of those used in ICF facilities induce the phase transformation of optical-grade synthetic silica into stishovite at optical breakdown. The importance of this laser-driven phase transformation resides in its implications in terms of laser-damage propagation in optics used in high-power photonics as the presence of stishovite enhances the coupling between the laser beam and the optical surface. Stishovite has a much higher refractive index ($n \sim 1.8$)²⁷ than silica ($n \sim 1.46$), and therefore introduces significant micro-lensing effects that create localized field enhancements that may exceed the LIDT of the surrounding material. More importantly, stishovite has the smallest bandgap (5.5 eV) of all SiO₂ polymorphs²⁸. The change from a three-photon to a two-photon absorption mechanism substantially lowers the threshold for multi-photon ionization at 355 nm, which is an important energy-absorption path for damage propagation. Furthermore, the observed presence of defects in the stishovite crystals is likely to create intra-gap absorbing states that will lower the LIDT of damaged fused silica at all wavelengths. Finally, first-principles calculations predict the formation of small amounts of octahedrally coordinated silicon in the compressed amorphous matrix²⁹, which will alter its optical properties on rapid quenching to ambient conditions by introducing local absorption centres. If damage propagation is indeed due to the formation of stishovite and octahedrally coordinated SiO₂ units in the silica matrix, transformation of the stishovite back into

tetrahedral SiO₂ glass may be the reason for the recent preliminary success of mild CO₂ laser annealing as a growth mitigation strategy³⁰.

METHODS

Damage was initiated on the front surface of a polished fused silica window with a 45 J cm⁻² laser burn from a frequency tripled Nd:YAG laser ($\lambda = 355 \text{ nm}$) with a 8.4-ns pulsewidth (FWHM) at a 10 Hz repetition rate. The 1/e² diameter of the gaussian laser beam was 1 mm. Repetitive irradiation at lower fluence caused laser drilling from the surface into the bulk of the window. Deposited material was found at the surface within the footprint of the plasma in a 1.5-mm radius around the entrance hole of the drilled channel, and was collected with a spatula prior to soaking in a diluted HF solution (5%) overnight. During the HF etching, tetrahedral SiO₂ dissolves in the acid leaving octahedral SiO₂ as a residue, according to the procedure published elsewhere¹⁷. The remaining material was rinsed and suspended in ethanol. A drop of the ethanol suspension was deposited on a copper grid coated with holey carbon suitable for TEM.

Synthetic silica from the same batch as the irradiated sample was ground to <1 μm grains for the infrared spectroscopy.

A synthetic stishovite pellet was prepared by hot isostatic compression of vitreous silica in a graphite furnace. The maximum grain size was of the order of 100 μm . The large grains provided essentially single-crystal infrared spectra.

TEM characterization was performed on a Philips CM200 FEG-(S)/TEM equipped with a field-emission gun and operating at 200 kV. Diffraction patterns were collected with nearly parallel illumination. No substantial change between patterns acquired within a few minutes was noticed. Stishovite amorphizes under a focused electron beam, therefore X-ray energy dispersive spectroscopy (EDS) using a focused probe was performed only after the diffraction patterns were acquired. Because of electron-beam irradiation damage and preferential oxygen sputtering, EDS only provided qualitative information. Aluminum and fluorine were detected as impurities but the interplanar spacings shown in Fig. 2b cannot be matched satisfactorily to alumina, nor to any of the known compound salts of aluminum and fluorine, in their anhydrous, hydroxylated and hydrated forms.

The infrared spectra were taken at the Advanced Light Source, Beamline 1.4 (Lawrence Berkeley National Laboratory) with a Nic-Plan 760 infrared microscope equipped with a liquid-nitrogen-cooled MCT-A detector connected to a Nicolet Magna 760 FTinfrared spectrometer. The radiation source was a 1,300 K thermal black body (Globar). The frequency range was 550 cm⁻¹ to 6,000 cm⁻¹. The scan resolution was 4 cm⁻¹. The spot diameter at the sample was approximately 100 μm .

SEM characterization was performed on a JEOL JSM 6340F field-emission microscope.

Received 23 January 2003; accepted 29 September 2003; published 2 November 2003.

References

1. Paisner, J. A. The national ignition facility project. *Fusion Technol.* **26**, 755–766 (1994).
2. Glanz, J. A harsh light falls on NIF. *Science* **277**, 304–305 (1997).
3. *Laser-Induced Damage in Optical Materials Collected papers 1960–1999* (SPIE, Bellingham, Washington, 1999).
4. Wong, J. et al. in *Laser-Induced Damage in Optical Materials* (eds Exarhos, G. J., Guenther, A. H., Lewis, K. L., Soileau, M. J. & Stolz, C. J.) 466–467 (SPIE 4347, Bellingham, Washington, 2000).
5. Stevens-Kalceff, M. A., Stetsmans, A. & Wong, J. Defects induced in fused silica by high fluence ultraviolet laser pulses at 355 nm. *Appl. Phys. Lett.* **80**, 758–760 (2002).
6. Salleo, A., Sands, T. & Génin, F. Y. Machining of transparent materials using an infrared and UV nanosecond pulsed laser. *Appl. Phys. A* **71**, 601–608 (2000).

7. Génin, F. Y., Salleo, A., Pistor, T. V. & Chase, L. L. Role of intensification by cracks in optical breakdown on surfaces. *J. Opt. Soc. Am. A* **18**, 2607–2616 (2001).
8. Stuart, B. C. *et al.* Optical ablation by high-power short-pulse lasers. *J. Opt. Soc. Am. B* **13**, 459–468 (1996).
9. Hofmeister, A. M., Xu, J. & Akimoto, S. Infrared spectroscopy of synthetic and natural stishovite. *Am. Mineral.* **75**, 951–955 (1990).
10. Williams, Q. & Jeanloz, R. Spectroscopic evidence for pressure-induced coordinated changes in silicate glasses and melts. *Science* **239**, 902–905 (1988).
11. Dubrovinsky, L. S. *et al.* Experimental and theoretical identification of a new high-pressure phase of silica. *Nature* **388**, 362–365 (1997).
12. El Goresy, A., Dubrovinsky, L., Sharp, T. G., Saxena, S. K. & Chen, M. A Monoclinic Post-Stishovite Polymorph of Silica in the Shergotty Meteorite. *Science* **288**, 1632–1634 (2000).
13. German, V. N., Podurets, M. A. & Trunin, R. F. Synthesis of a high-density phase of silicon dioxide in shock waves. *Sov. Phys. -JETP* **37**, 107 (1973).
14. Haines, J., Leger, J. M., Gorelli, F. & Hanfland, M. Crystalline post-quartz phase in silica at high pressure. *Phys. Rev. Lett.* **87**, 155503 (2001).
15. Kingma, K. J., Mao, H. K. & Hemley, R. J. Synchrotron X-Ray diffraction of SiO₂ to multimegabar pressures. *High Press. Res.* **14**, 363–374 (1996).
16. Liu, L. G., Bassett, W. A. & Sharpy, J. New high-pressure modifications of GeO₂ and SiO₂. *J. Geophys. Res.* **83**, 2301–2305 (1978).
17. Kleeman, J. D. & Ahrens, T. J. Shock-induced transition of quartz to stishovite. *J. Geophys. Res.* **78**, 5954–5960 (1973).
18. Teter, D. M., Hemley, R. J., Kresse, G. & Hafner, J. High pressure polymorphism in silica. *Phys. Rev. Lett.* **80**, 2145–2148 (1998).
19. Dean, P. The vibrational properties of disordered systems: numerical studies. *Rev. Mod. Phys.* **44**, 127–168 (1972).
20. Almeida, R. M. Detection of LO modes in glass by infrared reflection spectroscopy at oblique incidence. *Phys. Rev. B* **45**, 161–170 (1992).
21. Hu, S. M. Infrared absorption spectra of SiO₂ precipitates of various shapes in silicon: Calculated and experimental. *J. Appl. Phys.* **51**, 5945–5948 (1980).
22. Salleo, A. *et al.* Energy deposition at front and rear surfaces during ps laser interaction with fused silica. *Appl. Phys. Lett.* **78**, 2840–2842 (2001).
23. Gratz, A. J., Deloach, L. D., Clough, T. M. & Nellis, W. J. Shock amorphization of cristobalite. *Science* **259**, 663–666 (1993).
24. Gratz, A. J. *et al.* Shock metamorphism of quartz with initial temperatures -170 to +1000 °C. *Phys. Chem. Min.* **19**, 267–288 (1992).
25. Fedoseev, D. V., Varshavskaya, I. G., Lavrant'ev, A. V. & Derjaguin, B. V. Phase transformations in highly dispersed powders during their rapid heating and cooling. *Power Technol.* **44**, 125–129 (1985).
26. Alam, M., DebRoy, T., Roy, R. & Breval, E. High-pressure phases of SiO₂ made in air by Fedoseev-Derjaguin laser process. *Appl. Phys. Lett.* **53**, 1687–1690 (1988).
27. Stishov, S. M. & Popova, S. V. New dense polymorphic modification of silica. *Geokhim.* **10**, 837–839 (1961).
28. Alvarez, J. R. & Rez, P. Electronic structure of stishovite. *Solid State Commun.* **108**, 37–42 (1998).
29. Trave, A., Tangney, P., Scandolo, S., Pasquarello, A. & Car, R. Pressure-induced structural changes in liquid SiO₂ from ab-initio simulations. *Phys. Rev. Lett.* **89**, 245504 (2002).
30. Brusasco, R. M., Penetrante, B. M., Butler, J. A. & Hrubesh, L. W. in *Laser-Induced Damage in Optical Materials* (eds Exarhos, G. J., Guenther, A. H., Lewis, K. L., Soileau, M. J. & Stolz, C. J.) 40–47 (SPIE, Bellingham, Washington, 2001).

Acknowledgements

Synthetic stishovite was provided by Baosheng Li at State University of New York, Stony Brook. Work performed at the National Center for Electron Microscopy and at the Advanced Light Source at Lawrence Berkeley National Laboratory was supported by the Director, Office of Science, Office of Basic Energy Sciences, Material Sciences Division of the US Department of Energy. The authors wish to thank Doreen Ah Tye for her help with the SEM analysis, William S. Wong and Kateri E. Paul for helpful discussions. Work by two of the authors (A.S. and F.Y.G.) was performed under the auspices of the US Department of Energy at Lawrence Livermore National Laboratory. Work by W.R. P. was partially supported by the National Science Foundation. Correspondence and requests for materials should be addressed to A.S.

Competing financial interests

The authors declare that they have no competing financial interests.